J Neuropathol Exp Neurol. Author manuscript; available in PMC 2010 February 04.

Published in final edited form as:
J Neuropathol Exp Neurol. 2006 June ; 65(6): 549–561.

High resolution array-based comparative genomic hybridisation of medulloblastomas and supra-tentorial primitive neuroectodermal tumours

Martin Gerard McCabe, MB/BChir[1], **Koichi Ichimura, PhD**[1], **Lu Liu, PhD**[1], **Karen Plant, MSc**[1], **L Magnus Bäcklund, MD PhD**[2], **Danita M Pearson, PhD**[1], and **Vincent Peter Collins, MD**[1]

[1] University of Cambridge Department of Pathology, Division of Molecular Histopathology

[2] Department of Oncology Pathology, The Karolinska Institute, Stockholm, Sweden

Abstract

Medulloblastomas and supratentorial primitive neuroectodermal tumours are aggressive childhood tumours. We report our findings using array comparative genomic hybridisation (CGH) on a whole-genome BAC/PAC/cosmid array with a median clone separation of 0.97Mb to study 34 medulloblastomas and 7 supratentorial primitive neuroectodermal tumours. Array CGH allowed identification and mapping of numerous novel small regions of copy number change to genomic sequence, in addition to the large regions already known from previous studies. Novel amplifications were identified, some encompassing oncogenes, *MYCL1*, *PDGFRA*, *KIT* and *MYB*, not previously reported to show amplification in these tumours. In addition, one supratentorial primitive neuroectodermal tumour had lost both copies of the tumour suppressor genes *CDKN2A* & *CDKN2B*. Ten medulloblastomas had findings suggestive of isochromosome 17q. In contrast to previous reports using conventional CGH, array CGH identified three distinct breakpoints in these cases: Ch 17: 17940393-19251679 (17p11.2, n=6), Ch 17: 20111990-23308272 (17p11.2-17q11.2, n=4) and Ch 17: 38425359-39091575 (17q21.31, n=1). Significant differences were found in the patterns of copy number change between medulloblastomas and supratentorial primitive neuroectodermal tumours, providing further evidence that these tumours are genetically distinct despite their morphological and behavioural similarities.

Keywords

Medulloblastoma; supratentorial primitive neuroectodermal tumour; array-CGH; genomic copy number

INTRODUCTION

Medulloblastoma is a highly malignant invasive embryonal tumour of the cerebellum and one of the most common solid tumours of childhood. Supratentorial primitive neuroectodermal tumour (stPNET) is a related tumour found in the cerebrum or suprasellar region (1). Current management of both tumours involves surgery, aggressive chemotherapy, and craniospinal radiotherapy. Long-term survival figures are generally poor

Corresponding author Martin G McCabe Department of Pathology, Division of Molecular Histopathology, Cambridge University, Box 231, Level 3 Lab Block, Addenbrooke's Hospital, Hills Road, Cambridge CB2 2QQ. UK Phone: +44 1223 762084 Fax: +44 1223 586670 mcm41@cam.ac.uk.

(around 60% 5-year survival). Furthermore, because the developing brain is exposed to therapy, debilitating long-term sequelae occur in the majority of cases. An increased understanding of the genetic and molecular mechanisms underlying the development of these tumours will lead to innovative treatments that specifically target the molecular abnormalities of the tumour cells.

Conventional cytogenetic and molecular genetic techniques, including conventional comparative genomic hybridisation (CGH), have uncovered some chromosomal abnormalities consistently found in these tumours. The most commonly reported single change, present in 30-50% of cases of medulloblastoma, is isochromosome 17q (i(17q)); losses on 8p, 10, 11, 16q, 17p, 19, 20, 22, X & Y and gains of 1q, 2p, 4q, 6q, 7, 9p, 13q, 17q & 18 are also reported to occur frequently (2-10). Relatively little is known of the biology of stPNETs. They were grouped in the same diagnostic category as medulloblastomas prior to the most recent WHO guidelines (1), and the two tumours continue to be treated along similar lines. However, although i(17q) is a frequent finding in medulloblastomas, its presence has not been documented in stPNETs, emphasizing that while embryonal tumours of the central nervous system may share similar morphology, they constitute a diverse group of genetically distinct tumour types (8; 11).

Although conventional CGH detects large regions of copy number change, the resolution of array-based CGH is far higher and is dependent primarily on the size and spacing of adjacent clones. In this study we use a 1Mb whole genome BAC/PAC/cosmid array to analyse a series of medulloblastomas and stPNETs. We report several novel amplifications, some of which encompass known oncogenes not previously known to be involved in medulloblastomas or stPNETs. We report novel non-random copy number changes. Additionally, because array CGH allows higher resolution than conventional CGH and karyotyping for the detection of boundaries between regions of normal and altered copy number, we are able to refine the boundaries of some known alterations.

MATERIALS AND METHODS

Patients, tumour tissue and DNA isolation

A total of 34 medulloblastoma samples from 32 patients were included in the analysis. Histopathological classification was according to the most recent WHO recommendations (1). All medulloblastomas were classic medulloblastomas; there were no desmoplastic or large-cell variants. In total, 31 samples were from primary tumours: three of these were from patients with metastatic disease at initial presentation whose metastases were not sampled (PM27, PM35, PM50). In addition, 2 samples were from the sites of relapsed disease (PM5 and PM17R); for one of these we had samples from initial presentation (PM17) and relapse (PM17R). One sample (PM13) was from a recurrent cerebral metastasis. For this patient we had tissue from primary tumour (PM33) and metastasis (PM13). At tumour resection the median age of the patients with medulloblastoma was 8.9 years (range 0.6 to 41.0 years). Also included were 7 cerebral PNETs, of which 2 were recurrent tumours. The patients with stPNET had median age 3.3 years (range 2.7 to 23 years). The tumours were resected at the Karolinska Hospital, Stockholm and the Sahlgrenska University Hospital, Gothenburg, Sweden, between 1987 and 1997. Tumour specimens were selected for DNA extraction following histological examination to ensure a minimum composition of 85% tumour cells.

DNA was extracted from frozen tumour pieces and blood lymphocytes as described previously (12). Tumour samples were stored at −135°C and blood was stored at −20°C prior to DNA extraction. Extracted DNA was stored at −80°C.

Construction of genomic arrays

The 1Mb array clone set was obtained from the Wellcome Trust Sanger Institute (13). An additional 43 BAC clones were added to the 1Mb clone set to give a higher clone density at certain genomic regions. *Drosophila* clones (n=6) were used to calculate background signal due to non-specific DNA binding. The complete list of clones used in analysis is described in Supplemental Data 1. Clone positions quoted are according to the NCBI 35 assembly of the human genome (Ensembl release 26.35.1, November 2004). Preparation of the array was based on the protocols used by the Wellcome Trust Sanger Institute, Cambridge, UK, with minor modifications ((13) and (14)). Briefly, clone DNA was extracted and amplified using three DOP primers. The 3 DOP-PCR products were mixed and amplified using a 5′-amine-modified universal primer. Amine-linked PCR products were arrayed onto amine-binding slides (CodeLink, Amersham Biosciences, Little Chalfont, Buckinghamshire, UK) in duplicate as described and stored at room temperature. Each array was composed of 24 blocks; *Drosophila* clones and clones from individual chromosomes were evenly distributed throughout all blocks.

Certain findings from the 1 Mb array were analysed in more detail using overlapping clones from the relevant chromosomal tiling path clone sets or 32k clone sets obtained from the Wellcome Trust Sanger Institute (listed in Supplemental Data 2). These were arrayed randomly throughout blocks in duplicate in conjunction with a whole-chromosome tiling path array composed of 16 blocks (data not shown). Clone preparation was as described above.

Labelling and hybridization to microarrays

Labelling and hybridisations were performed essentially as we have described previously (14). Briefly, 400 ng of test and reference DNA were labelled using a Bioprime Labelling Kit (Invitrogen, Carlsbad, CA) with a modified dNTP reaction mixture as previously described. Test DNA was hybridized with sex-mismatched reference DNA from samples of pooled blood from 20 normal males or 20 normal females. The labelled and purified test and reference DNA were mixed and co-precipitated with 45μg Cot1 DNA (Roche Diagnostics, Mannheim, Germany). The precipitated DNA was dissolved in hybridisation buffer, incubated at 37°C for 2 hours and hybridised to the array which had been pre-hybridised with 400μg herring sperm DNA (Sigma-Aldrich, St Louis, MO) and 80μg Cot1 DNA. Arrays were allowed to hybridise for up to 48 hours at 37°C then washed as described.

Array analysis

Arrays were scanned and analysed as described elsewhere (14). In control normal male/normal female hybridisations (n=6), fluorescence ratios were found to follow a roughly normal distribution about their mean value. Therefore, our threshold for making single copy loss and gain decisions was three standard deviations from the mean ratio, equivalent to a $\log_2$ ratio of −0.21 for loss and +0.18 for gain. Furthermore, clones whose $\log_2$ ratios exceeded these threshold values in normal-normal hybridisations were permanently excluded from the array. Following the removal of these clones, other clones were excluded on an array-by-array basis. Briefly, for each array, any spot with an intensity in the Cy3 channel (reference) of less than quadruple the average intensity of 6 Drosophila BAC spots was excluded from analysis. Spots were also excluded if there was overlying artefact, poor morphology or a difference in ratios of greater than 10% between duplicates. The choice of 10% difference between duplicates was arbitrary and led to the exclusion of a median of 1 clone (range 0 – 29) per array. This and the other stated reasons for spot exclusion could potentially lead to a reduction in array resolution. Therefore, arrays were repeated if more than 5% of spots were excluded. Following repeats, a maximum of 4.3% of spots were excluded per sample (mean 3.4%, range 1.3 – 4.3%). For the remaining non-excluded spots,

local background intensity was subtracted from the median foreground intensity for each channel, fluorescence ratios were calculated for each spot and the ratios of duplicate spots were averaged. To control for spatial variation across the slides, a print-tip block normalization to the median percentile was performed by calculating the median test/reference spot intensity ratio for each block and dividing individual averaged clone test/reference ratios by this value. Because the majority of hybridisations were sex-mismatched (the exceptions were repeat hybridisations with constitutional DNA from the same patient to confirm somatic copy number changes), decisions on copy number change were confined to autosomal clones. The results were analysed using plots of $\log_2$ normalised Cy5:Cy3 intensity ratios (ordinate) against clone position (abscissa).

Our threshold $\log_2$ ratios for judging copy number change (based on normal diploid samples) were −0.21 for loss and +0.18 for gain. In some cases clones showing $\log_2$ ratios less than these threshold values were also scored as showing loss or gain if the $\log_2$ ratios of several adjacent clones were visibly different from the baseline $\log_2$ ratio for that sample. A near-triploid sample showing single copy loss or gain of a locus would be expected to have $\log_2$ ratios of −0.58 and +0.42 respectively for the lost and gained regions. A near-tetraploid sample would be expected to show $\log_2$ ratios of −0.42 and +0.32 respectively for single copy loss and gain. In both cases, these values fall outside of our threshold, allowing us to judge single copy loss and gain in all variations of DNA ploidy frequently seen in medulloblastomas and stPNETs. In the normal-normal hybridisations the median $\log_2$ ratio of all autosomal clones was zero. Due to the difference in the number of X chromosomes between male (single copy) and female (2 copies), chromosome X clones displayed a median $\log_2$ ratio between −0.55 and −0.67 for male (test) versus female (reference) hybridisations (see Figure 1) and +0.66 to +0.67 for female (test) versus male (reference) hybridisations. These values lay outside our threshold values of −0.21 for judging loss and +0.18 for gain, demonstrating the ability of our array to detect single copy loss and gain.

With each revision of the human genome assembly, mapping position of a proportion of clones is changed. Therefore, clones mapped to multiple locations under the NCBI 35 assembly and those displaying an inconsistent $\log_2$ ratio compared to neighbouring clones in multiple cases were considered unreliable and were excluded. Following exclusion of these unrelieable clones and clones whose $\log_2$ ratios exceeded the threshold values in normal-normal hybridisations, 3038 clones were used in analysis (2555 BACs, 477 PACs and 6 cosmids). Clones varied in size between 0.141 kb and 288 kb (mean clone size 152 kb). The mean mid-clone separation was 0.97 Mb. In reality this does not translate into the actual resolution across the whole array because of the irregular spacing of clones and the size of individual clones. Some regions, primarily centromeres, had a mid-clone separation significantly greater than 0.97 Mb. However, the separation was less than 1 Mb in 61.4% of adjacent clones, less than 2 Mb in 94.2% of adjacent clones and less than 3 Mb in 98.4% of adjacent clones.

The majority of regions showing copy number change involved several adjacent clones. However, in some cases, single clones showed copy number alterations without neighbouring clones showing similar change. To decide which of these single clone changes were due to germline variation, a set of hybridisations (n=6) was performed comparing tumour DNA and constitutional DNA from the same patient. In the case of germline variation these single clone copy number changes disappeared because they were present both in tumour and constitutional DNA. Of all loci affected by single clone copy number alteration (n=170), we analysed 70 against constitutional DNA from the same patient: 7 of these 70 loci (10%) revealed germline copy number change (affected clones are listed in Supplementary Data 3). The majority of single clone changes were found to be reproducible on repeat hybridisations (repeat hybridisations were carried out for several reasons

including: to confirm certain changes such as homozygous deletions and high-level amplifications; to confirm certain single clone changes seen in multiple cases; to correct technically poor initial hybridisations). Single clone changes that were not reproducible are not reported.

Homozygous loss was judged if clones showed a $\log_2$ ratio of greater amplitude than −1.0. High-level amplifications were judged if clones had a $\log_2$ ratio of greater than +1.0 or ≥ 1.0 more than that of the other clones for that chromosome if occurring on a chromosome exhibiting copy number gain. In practice all amplifications were surrounded by genome of normal copy number except for two amplifications on chromosome 2 for PM34, where the amplicon $\log_2$ ratios were more than 30x the surrounding copy number gain. Copy number was estimated where appropriate (for instance in assessing degree of amplification) by multiplying the unlogged fluorescence ratio by modal copy number. A modal copy number of 2 was assumed for those cases where this was not known from interphase FISH experiments.

Microsatellite analysis

Microsatellite analysis was performed as described previously (15) using 9 markers from both arms of chromosome 6: *D6S470*, *D6S429*, *D6S260*, *D6S276*, *D6S430*, *D6S1572*, *D6S441*, *D6S415*, *D6S1581* and 8 markers from both arms of chromosome 17: *D17S849*, *D17S947*, *D17S921*, *D17S975*, *D17S932*, *D17S790*, *D17S794*, *D17S929*. The primer sequences were those publicly available (http://www.ensembl.org/Homo_sapiens).

Interphase fluorescent in situ hybridisation

In cases for which formalin-fixed paraffin-embedded tissue was available, interphase fluorescent in situ hybridisation (I-FISH) was performed primarily to identify a chromosome with an absolute copy number of 2 in each case, thereby providing an anchor against which to perform supervised copy number analysis. In addition we used I-FISH to confirm certain copy number changes suggested by array CGH. Based on the array CGH results, chromosomes 7, 10, 17 and 18 were chosen to fulfil these purposes. A tissue microarray was constructed as follows. Cores (n=4 for each case) of 0.6mm diameter were taken from areas identified on haematoxylin and eosin-stained sections to be representative tumour tissue from 6 medulloblastomas and 2 stPNETs and arrayed into a fresh paraffin block using a manual tissue arrayer (Beecher Instruments, Silver Spring, MD, USA). Five-micrometer sections from the array were placed on positively charged slides and dried overnight at 37°C. Following de-waxing in xylene and dehydration in 100% ethanol, the slides were pre-treated in 1M sodium thiocyanate at 72°C for 10 minutes and washed briefly in 2×SSC. Protein digestion in Proteinase K (200μg/ml, 45°C) was performed for 45 minutes. The slides were washed in 2×SSC and dual colour FISH reactions were performed using commercial centromeric alpha satellite probes. FISH probes for chromosomes 7 (spectrumOrange) and 17 (spectrumGreen) in combination and for chromosomes 10 (spectrumOrange) and 18 (spectrumGreen) in combination were assessed (Vysis, Downers Grove, IL, USA). Probe hybridisation was performed according to the manufacturer's instructions. The slides were counterstained with VECTASHIELD® HardSet Mounting Medium with DAPI (Vector Laboratories, Peterborough, UK). Nuclei were viewed using a Zeiss Axiophot epifluorescence microscope equipped with a ×63 oil immersion objective and filter sets for DAPI, spectrumOrange and FITC. Normal ranges were based on figures obtained by counting 500 nuclei of normal cerebral grey and white matter.

Semi-quantitative Multiplex PCR

Primers for part of exon 2 of *MYCL1* (forward primer TGACTGCGGGGAGGATTTCTAC; reverse primer

CGTATGATGGAGGCGTAGTTCCTG), part of exon 3 of *PDGFRA* (forward primer TCATCCTTTTCTCTGAGATGCTTTG; reverse primer GCCTTCAAGCTCATTCTCTTCTGTC) or part of exon 15 of *MYB* (forward primer GGGAGTTCTGCATTTGATCCG; reverse primer GCTACAAGGCAGTAAGTACACCGTC), together with primers for a control locus (D2S1743, forward primer ATGCAGGTTTGGCCATTC; reverse primer ATGAACCCAGGTGGTGTCAT) were used in a multiplex PCR. The multiplex reactions included 250 μM of each dNTP, 2.0 mM (*MYCL1* and *MYB* reactions) or 2.5 mM (*PDGFRA* reaction) $MgCl_2$, 25 mM DMSO (*MYCL1* reaction only), the appropriate test primer concentration (*1.5* μM for *MYCL1*, 0.5 μM for *PDGFRA* and *MYB*), the appropriate control primer concentration (0.25 μM for *MYCL1* reaction, 0.5 μM for *PDGFRA* and *MYB* reactions), 0.5 U Thermostart® DNA polymerase and reaction buffer supplied by the manufacturer (ABgene UK, Epson, UK) and 10 ng of DNA template in a 20 μl reaction. We had previously optimised reaction conditions and had shown a near-linear relationship between template and product at cycle numbers of around 28. PCR conditions were as follows: initial denaturation at 94 °C for 10 mins; 94 °C for 30 seconds, 55 °C for 30 seconds, 72 °C for 30 seconds for 28 cycles; final extension at 72 °C for 5 minutes. PCR product was run on a 3% agarose gel containing ethidium bromide 500 μg/l. Images were viewed using a GelDoc-It Imaging System (Ultra-Violet Products Ld, Cambridge, UK) and band intensities analysed using the manufacture's analysis software. One multiplex reaction for each test locus was performed using normal control DNA as a template. Copy number was estimated using the formula:

$$\text{Copy number} = 2 \times \frac{(\text{Text locus intensity / control locus intensity (test DNA)})}{(\text{Text locus intensity / control locus intensity (control DNA)})}$$

where test locus = *MYCL1*, *PDGFRA* or *MYB* and control locus = D2S1743.

Statistical analysis

Fisher's exact test was used to compare the frequency of specific findings between medulloblastomas and stPNETs.

RESULTS

Array Comparative Genomic Hybridisation of Medulloblastomas

In total, 34 medulloblastomas were analysed using our 1Mb whole genome BAC/PAC/cosmid array. The medulloblastomas had a median of 13 alterations in copy number per sample (range 2 to 28). The complete list of normalised $\log_2$ ratios for each case are given in Supplemental Data 1.

Three high-level amplifications were seen in two tumours. All amplicons were confirmed using semi-quantitative multiplex PCR and/or array CGH using tiling path arrays of the region. The PCR quantitation and tile-path array results are summarised in Table 1. Two amplicons in medulloblastomas encompassed known oncogenes, *MYCN* and *MYCL1*. High-level amplification of *MYCL1* is a novel finding in medulloblastomas. The first tumour, PM22, had amplification of 2 adjacent clones RP1-118J21 and RP4-739H11, Ch 1: 39894236-40857027 (1p34.2). The amplified clones encompassed *MYCL1* and were surrounded by the non-amplified clones RP11-113D13 and RP11-342M1. Semi-quantitative multiplex PCR confirmed amplification of the *MYCL1* gene. Further examination of the *MYCL1* region using a tile-path array revealed a 3.31 Mb amplicon extending from clone RP1-110F11 to RP5-994D16, Ch 1: 39720241- 42788785 (Figure 2). The second tumour,

PM34, had two discrete amplicons, both involving chromosome 2. Further analysis **(**Table 1**)** revealed the first amplicon identified by the 1 Mb array to contain only the genes *MYCN* and *MYCNOS* (Ch 2: 15965376- 16196294). However, the second amplicon consisted of two small adjacent amplicons. Ch 2: 41659940-42030267 and Ch 2: 42317971-42576890 (Figure 3).

Medulloblastomas displayed several consistent copy number changes. The frequency of gain and loss of individual clones is shown in Figure 4. Gain of chromosome 17: 50112652-78374826 was the most common aberration, present in 20 of 34 cases (59%). All cases with loss of 17p also had gain of 17q. The converse was not true however; some cases showed gain of 17q without loss of 17p (n=3) or gain of the whole of chromosome 17 (n=5). In those cases with findings suggestive of isochromosome 17q (loss of 17p and gain of 17q), array CGH identified three distinct breakpoints, illustrated in Figure 5. The breakpoint found most frequently, between clones RP11-189D22 and RP1-162E17 (Ch 17: 17940393-19251679, 17p11.2) was seen in 6 cases. Four cases had a peri-centromeric breakpoint, between RP11-121A13 and RP11-138P22, Ch 17: 20111990-23308272 (17p11.2-17q11.2). The remaining case had a breakpoint between clones RP11-948G15 and RP11-392O1, Ch 17: 38425359-39091575 (17q21.31).

Several regions besides 17q frequently showed copy number gain, including the novel finding of gain of a region on Ch 19: 38091322-63771717 extending from RP11-298M15 to PAC1129C9 (19q13.11-19q13.43) in 6 cases (18%). The regions most commonly lost and gained are listed in Table 2. In each case we were able to delineate precisely the affected region relative to genomic sequence.

Array Comparative Genomic Hybridisation of Supratentorial Primitive Neuroectodermal Tumours

StPNETs (n=7) had a median of 16 copy number alterations per sample (range 7 to 30). Amplifications were found in 3 of 7 tumours and one case had a homozygous deletion. The complete list of $\log_2$ ratios each case is described in Supplemental Data 1.

The three tumours with amplifications showed 5 separate amplified regions, described in Table 1. PM3 had a single amplicon at Ch 4: 53711035-55501429, encompassing the oncogenes *PDGFRA* and *KIT*. Case PM36 had 3 separate amplicons, all on chromosome 6: Ch 6: 1281096-1530520 ; Ch 6: 134963006-136135904 including the oncogene *MYB*; and Ch 6: 143821730-144578075. Case PM51 had amplification of Ch 19: 59127814-59464094.

The most frequent finding in the stPNETs was loss of clone RP11-245B11 at Ch 13: 113770458-113954546, present in 4 cases (57%). While case PM 21 showed loss of the whole of 13q and PM 3 lost a 75 Mb region from 13q14.11 to 13qter, cases PM 36 & PM 51 had lost only clone RP11-245B11. This specific loss of RP11-245B11 was reproducible in both cases and the spots had good morphology and strong signal. The frequency of loss and gain of all individual clones is shown in Figure 4.

Case PM 20 showed homozygous loss of a single clone, RP11-145E5 ($\log_2$ ratio −2.21) encompassing the *CDKN2A* and *CDKN2B* genes, illustrated in Figure 6. The homozygously deleted clone was surrounded by a 0.4Mb region of single copy loss defined by clones RP11-149I2 to RP11-408N14. This homozygous loss remained apparent when tumour DNA was re-hybridised using constitutional DNA from the same patient as reference, discounting the possibility of a deletion polymorphism at this site.

Verification of Modal Copy Number

Because CGH demonstrates relative, rather than absolute, copy number (relative to the modal sample copy number), we used I-FISH to determine modal copy number in a subset of cases arrayed onto a tissue microarray using alpha satellite probes for the centromeres of chromosome 7, 10, 17 and 18. In all but one sample (PM 35), a $\log_2$ ratio of zero at peri-centromeric clones on array CGH corresponded to a copy number of 2 for that centromere on I-FISH, , implying a modal copy number of 2 for the sample.. For all cases where I-FISH showed centromeric copy number gain, array CGH also showed copy number gain of the peri-centromeric clones. In one case (PM 35), approximately equal numbers of clones had $\log_2$ ratios of 0 and −0.4 (illustrated in Figure 7). I-FISH showed regions with a $\log_2$ ratio of −0.4 on array CGH to have disomy; all other genomic regions had copy number gain. .

Comparison of Array Comparative Genomic Hybridisation Results with Microsatellite Analysis

A series of dinucleotide repeat microsatellite analyses was performed using sixteen loci representing both arms of chromosomes 6 and 17. These were used to analyse a subset of samples (n=11) for which constitutional DNA was available At all informative loci, the findings of microsatellite analysis and array CGH were in agreement: single copy loss and gain detected by array CGH was associated with allelic imbalance of microsatellite loci while normal copy number detected by array CGH was associated with allelic balance of microsatellite loci. While allelotyping could not distinguish allelic loss from allelic gain, however, array CGH clearly differentiated the two (Figure 8).

Comparison of Medulloblastomas and Supratentorial Primitive Neuroectodermal Tumours

Fisher's exact test was used to compare copy number changes between medulloblastomas and stPNETs. Despite the small number of stPNETs in our series, we found some changes to show statistically significant differences in occurrence between the tumour groups. Gain of 17q was significantly more common in medulloblastomas (20 of 34) than in stPNETs (0 of 7) (p-value = 0.00862). Loss of the telomeric end of 13q was more common in stPNETs (4 of 7) than medulloblastomas (1 of 34) (p-value = 0.00162). No other specific copy number changes were different between the two groups. However, stPNETs were significantly more likely to have amplifications (3 of 7) than medulloblastomas (2 of 34) (p-value = 0.02782). These estimates of statistical significance do not reflect a Bonferroni correction for multiple testing.

DISCUSSION

The benefits of array CGH over metaphase CGH include the ability to examine many regions of the genome at high resolution in one experiment and the capacity to map regions of copy number loss and gain to genome sequence (16-18). Using array CGH we have identified several novel findings in these tumours. These include amplifications, some encompassing known oncogenes not previously reported to be involved in medulloblastomas and stPNETs and frequent copy number changes not previously described. Furthermore, the increased resolution afforded by array CGH has allowed us to delineate previously reported regions of copy number change more precisely. Finally, we have contributed to the growing evidence that medulloblastomas and stPNETs, while morphologically similar, are genetically distinct.

We are the first to report high-level amplification of *MYCL1* in medulloblastomas and *PDGFRA, KIT* and *MYB* in stPNETs. Using conventional CGH, Russo et al (8) and Michiels et al (19) have reported medulloblastomas (2 of 43 and 1 of 15 respectively) with high-level gain at 1p34. In the case we report here with *MYCL1* amplification, array CGH

allowed us to delineate our amplicon boundaries precisely, identifying specific genes contained within the amplicon. Initial array CGH at 1Mb resolution showed an amplicon at 1p34. An overlapping tile-path array of the region identified a 3.31 Mb amplicon containing 80 genes including the growth factors *BMP8B* and *EDN2,* the gene for the basic helix-loop-helix protein HEYL and the transcriptional regulators *NFYC*, *CITED4* and *FOXJ3* in addition to the known oncogene *MYCL1*. In the only previous study to examine amplification status of *MYCL1* in medulloblastomas, Tong et al reported single copy gain but not high-level amplification (20). While *MYCN* amplification has been linked to poor prognosis in medulloblastomas, the significance of *MYCL1* amplification and/or over-expression is unknown. The case we report with *MYCL1* amplification was still alive at most recent follow up, more than 8 years from diagnosis. Case PM 34, however, with amplification of *MYCN*, succumbed to disease within one year.

Array CGH has identified genes co-amplified with *PDGFRA* and *KIT*. Sihto et al previously reported one medulloblastoma with amplification of the chromosome 4 centromere and high-level amplification of *KIT* (21). Although not specifically examined, it is likely that *PDGFRA* was co-amplified in that case given its proximity to both loci. Tong et al reported single copy gain but no high-level amplification of *PDGFRA* or *KIT* (20). Using conventional CGH, Russo et al reported one stPNET with high-level gain at 4q12-13 (8). In our study, array CGH has allowed more accurate delineation of the amplicon. Initially, 1 Mb-resolution array CGH of case PM 3 showed an amplicon with maximum size 3.6 Mb. Subsequent tile-path array CGH of the region revealed a 1.81 Mb amplicon containing 7 genes including the E3 ubiquitin ligase *LNX* in addition to co-amplification of *PDGFRA* and *KIT*. Over-expression of *PDGFRA* and *PDGFRB* has been reported to occur more frequently in metastatic than non-metastatic medulloblastomas and to be associated with worse prognosis (22; 23). On the contrary, the importance of *PDGFRA* expression and its relationship to metastatic disease in stPNETs is unknown. Case PM 3 had a non-metastatic stPNET and was still alive at last follow up 10 years following surgery. . (21)*MYB* amplification has not been reported in either tumour although described in other tumour types (24; 25). A tile-path array of the region surrounding the single amplified clone RP1-32B1 in case PM 36 revealed a 1.05 Mb amplicon containing *AHI1*, a gene known to be involved in cerebellar development in addition to the known oncogene *MYB*. Finally, in all but one amplicon we have reported the co-amplification of several genes. We are currently undertaking further analysis to identify the targeted gene(s) in each case.

A novel finding in our series was gain of 19q in medulloblastomas, present in 6 of 34 samples (18%). Although this has been described in a variety of different tumour types, including glioblastoma, oesophageal squamous cell carcinoma and ovarian carcinoma (26-28), it has not previously been reported to occur commonly in medulloblastomas. To date, no specific targeted genes have been identified in tumour types commonly exhibiting gain of 19q.

Array CGH allowed us to define the boundaries of all regions of copy number change and to map them to the genome. Three regions are particularly worthy of comment in the medulloblastomas (detailed in Table 2). The first two (8p and 20q) had regions of copy number loss of gradually reducing size in different samples, leading in each case to a small, commonly deleted region. The third region is the breakpoint of i(17q).

Loss of 8p has been described using conventional CGH, karyotyping and SKY. Most commonly loss of the whole arm or the whole chromosome is reported; single tumours have been reported with loss of 8p16, 8p21 & 8p23 by conventional CGH or karyotyping(3; 7; 19). In our series, three medulloblastomas had single copy loss of all of 8p; a further five tumours had lost smaller regions within 8p. The commonly deleted region extended from

RP5-991O23 to RP11-177H13, Ch 8: 5326020-23286627 (8p21.3-8p23.2) and shares some overlap with a commonly deleted region identified previously in medulloblastomas by Yin et al from 8p22-23.2 using allelotyping techniques (29). Yin et al describe two cases that showed a small area of homozygous loss adjacent to the tumour suppressor gene *DLC1.* While transcriptional loss of *DLC1* through deletion or promoter hypermethylation has been described in a variety of tumours including non small cell lung cancer, gastric and hepatocellular carcinoma (30-32), its methylation status in medulloblastomas is unknown.

We identified a commonly deleted region on 20q extending from RP5-1010E17 to RP13-152O15, Ch 20: 53411914-62163452 (20q13.2-13.33). Loss of the whole of 20q has been reported in various studies of medulloblastomas (3; 19). In our series 5 of 34 medulloblastomas had single copy loss of the whole of chromosome 20. Two further tumours had lost smaller regions within 20q. Hui et al recently reported frequent single copy gain of a region extending from 20q13.31 to 20q13.33, a region closely resembling our commonly lost region, in their series of 16 medulloblastomas using a genomic BAC array containing 1803 clones (33). While they conclude that gain of this region may have been underestimated previously by lower resolution studies using conventional CGH, it is interesting that our study utilising a higher resolution 3038-clone array has not only not identified gain, but has identified loss of the same region to be a common finding. Germline genetic differences between the two populations may partly explain the inconsistency between the two series. The same group have previously reported loss of 20q to occur consistently in ependymomas (34). Tong et al also describe a minimal deleted region at 20q13.2-13.3 in ependymomas using microsatellite repeat markers (35). This region overlaps with our minimal deleted region on 20q. In those reporting 20q loss, targeted genes have not been identified.

Various minimal commonly deleted regions on 17p have been reported using allelotyping methods (11; 36). However, although i(17q) is one of the most common findings in every series of medulloblastoma for which karyotypic alterations have been reported, few have studied the breakpoint region. In our series, three discrete breakpoints were seen. Of these, the two breakpoints accounting for the majority of cases, Ch 17: 17940393-19251679 (n=6) and Ch 17: 20111990-23308272 (n=4), matched precisely with two breakpoint cluster regions described by Scheurlen et al in cases with medulloblastoma, non-Hodgkin's lymphoma, acute myeloid leukaemia and chronic myeloid leukaemia blast crisis (CML-BC) using microsatellite markers (37). We are currently producing a tiled path array of chromosome 17 which will define the breakpoints in more detail and allow us to see specifically which gene(s) are affected.

Despite the small number of stPNETs in our series, statistically significant differences were observed between the two tumour types in the frequency of 17q gain and 13q loss, in addition to the observation that amplifications were more common in stPNETs. The tumours are both classed as primitive neuro-ectodermal tumours. However, while their treatment is similar, the prognosis for stPNETs is worse than that for medulloblastomas (38). There is already evidence that the two tumour types are genetically distinct (8; 11). Our data would strongly support the hypothesis that these tumours represent biologically separate entities and it is likely that the underlying molecular dissimilarities are responsible in part for the discrepancies in reported survival figures.

In conclusion, this is the highest resolution report to date of a genome-wide analysis of genomic copy number changes in medulloblastomas and stPNETs using array CGH. We have reported several novel amplicons, some of which include known oncogenes. We have accurately defined consistent copy number changes, including novel loci previously not reported to show consistent change. We have identified more precisely the positions of the

breakpoint in cases with i(17q). Finally, we have added to the evidence that medulloblastomas and stPNETs are separate biological entities, explaining to some degree their different outcome following treatment.

Supplementary Material

Refer to Web version on PubMed Central for supplementary material.

Acknowledgments

The authors thank Mr David Jones for performing interphase FISH on specimens of normal grey and white matter and Mr John Brown for technical assistance in the production of the tissue microarrays. The authors also thank the Centre for Microarray Resources at Cambridge University Department of Pathology for printing the arrays on which the paper is based. All clones were supplied by the Wellcome Trust Sanger Institute Archives Group (http://www.sanger.ac.uk/Teams/Team38/)

Financial support

M G McCabe was supported by a Clinical Research Training Fellowship from Cancer Research UK and by a grant from The Addenbrooke's Charities.

L Liu was supported by a grant from the Samantha Dickson Research Trust.

Authors were also supported by grants from CAMPOD, Cancer Research UK, The Jacqueline Seroussi Memorial Foundation for Cancer Research and The Ludwig Institute for Cancer Research.

REFERENCES

1. Giangaspero, F.; Bigner, SH.; Kleihues, P., et al. Chapter 8: ‘Embryonal Tumours’. In: Kleihues, K.; Cavenee, WK., editors. World Health Organization Classification of Tumours ‘Pathology and Genetics of Tumours of the Nervous System’. IARC Press; Lyon: 2000. p. 123-148.
2. Avet-Loiseau H, Venuat AM, Terrier-Lacombe MJ, et al. Comparative genomic hybridization detects many recurrent imbalances in central nervous system primitive neuroectodermal tumours in children. Br J Cancer. 1999; 79:1843–7. [PubMed: 10206302]
3. Bayani J, Zielenska M, Marrano P, et al. Molecular cytogenetic analysis of medulloblastomas and supratentorial primitive neuroectodermal tumors by using conventional banding, comparative genomic hybridization, and spectral karyotyping. J Neurosurg. 2000; 93:437–48. [PubMed: 10969942]
4. Gilhuis HJ, Anderl KL, Boerman RH, et al. Comparative genomic hybridization of medulloblastomas and clinical relevance: eleven new cases and a review of the literature. Clin Neurol Neurosurg. 2000; 102:203–209. [PubMed: 11154805]
5. Jay V, Squire J, Bayani J, et al. Oncogene amplification in medulloblastoma: analysis of a case by comparative genomic hybridization and fluorescence in situ hybridization. Pathology. 1999; 31:337–44. [PubMed: 10643003]
6. Nicholson J, Wickramasinghe C, Ross F, et al. Imbalances of chromosome 17 in medulloblastomas determined by comparative genomic hybridisation and fluorescence in situ hybridisation. Mol Pathol. 2000; 53:313–9. [PubMed: 11193050]
7. Reardon DA, Jenkins JJ, Sublett JE, et al. Multiple genomic alterations including N-myc amplification in a primary large cell medulloblastoma. Pediatr Neurosurg. 2000; 32:187–91. [PubMed: 10940769]
8. Russo C, Pellarin M, Tingby O, et al. Comparative genomic hybridization in patients with supratentorial and infratentorial primitive neuroectodermal tumors. Cancer. 1999; 86:331–9. [PubMed: 10421270]
9. Eberhart CG, Kratz JE, Schuster A, et al. Comparative genomic hybridization detects an increased number of chromosomal alterations in large cell/anaplastic medulloblastomas. Brain Pathol. 2002; 12:36–44. [PubMed: 11770900]

10. Shlomit R, Ayala AG, Michal D, et al. Gains and losses of DNA sequences in childhood brain tumors analyzed by comparative genomic hybridization. Cancer Genet Cytogenet. 2000; 121:67–72. [PubMed: 10958944]
11. Burnett ME, White EC, Sih S, et al. Chromosome arm 17p deletion analysis reveals molecular genetic heterogeneity in supratentorial and infratentorial primitive neuroectodermal tumors of the central nervous system. Cancer Genet Cytogenet. 1997; 97:25–31. [PubMed: 9242214]
12. Ichimura K, Schmidt EE, Goike HM, et al. Human glioblastomas with no alterations of the CDKN2A (p16INK4A, MTS1) and CDK4 genes have frequent mutations of the retinoblastoma gene. Oncogene. 1996; 13:1065–72. [PubMed: 8806696]
13. Fiegler H, Carr P, Douglas EJ, et al. DNA microarrays for comparative genomic hybridization based on DOP-PCR amplification of BAC and PAC clones. Genes Chromosomes Cancer. 2003; 36:361–74. [PubMed: 12619160]
14. Seng TJ, Ichimura K, Liu L, et al. Complex chromosome 22 rearrangements in astrocytic tumors identified using microsatellite and chromosome 22 tile path array analysis. Genes Chromosomes Cancer. 2005
15. Miyakawa A, Ichimura K, Schmidt EE, et al. Multiple deleted regions on the long arm of chromosome 6 in astrocytic tumours. Br J Cancer. 2000; 82:543–9. [PubMed: 10682663]
16. Pinkel D, Segraves R, Sudar D, et al. High resolution analysis of DNA copy number variation using comparative genomic hybridization to microarrays. Nat Genet. 1998; 20:207–11. [PubMed: 9771718]
17. Hurst CD, Fiegler H, Carr P, et al. High-resolution analysis of genomic copy number alterations in bladder cancer by microarray-based comparative genomic hybridization. Oncogene. 2004
18. Solinas-Toldo S, Lampel S, Stilgenbauer S, et al. Matrix-based comparative genomic hybridization: biochips to screen for genomic imbalances. Genes Chromosomes Cancer. 1997; 20:399–407. [PubMed: 9408757]
19. Michiels EM, Weiss MM, Hoovers JM, et al. Genetic alterations in childhood medulloblastoma analyzed by comparative genomic hybridization. J Pediatr Hematol Oncol. 2002; 24:205–10. [PubMed: 11990307]
20. Tong CY, Hui AB, Yin XL, et al. Detection of oncogene amplifications in medulloblastomas by comparative genomic hybridization and array-based comparative genomic hybridization. J Neurosurg. 2004; 100:187–93. [PubMed: 14758948]
21. Sihto H, Sarlomo-Rikala M, Tynninen O, et al. KIT and platelet-derived growth factor receptor alpha tyrosine kinase gene mutations and KIT amplifications in human solid tumors. J Clin Oncol. 2005; 23:49–57. [PubMed: 15545668]
22. Gilbertson RJ, Clifford SC. PDGFRB is overexpressed in metastatic medulloblastoma. Nat Genet. 2003; 35:197–8. [PubMed: 14593398]
23. MacDonald TJ, Brown KM, LaFleur B, et al. Expression profiling of medulloblastoma: PDGFRA and the RAS/MAPK pathway as therapeutic targets for metastatic disease. Nat Genet. 2001; 29:143–52. [PubMed: 11544480]
24. Edwards J, Krishna NS, Witton CJ, et al. Gene amplifications associated with the development of hormone-resistant prostate cancer. Clin Cancer Res. 2003; 9:5271–81. [PubMed: 14614009]
25. Hui AB, Lo KW, Teo PM, et al. Genome wide detection of oncogene amplifications in nasopharyngeal carcinoma by array based comparative genomic hybridization. Int J Oncol. 2002; 20:467–73. [PubMed: 11836556]
26. Burton EC, Lamborn KR, Feuerstein BG, et al. Genetic aberrations defined by comparative genomic hybridization distinguish long-term from typical survivors of glioblastoma. Cancer Res. 2002; 62:6205–10. [PubMed: 12414648]
27. Sham JS, Tang TC, Fang Y, et al. Recurrent chromosome alterations in primary ovarian carcinoma in Chinese women. Cancer Genet Cytogenet. 2002; 133:39–44. [PubMed: 11890988]
28. Yen CC, Chen YJ, Lu KH, et al. Genotypic analysis of esophageal squamous cell carcinoma by molecular cytogenetics and real-time quantitative polymerase chain reaction. Int J Oncol. 2003; 23:871–81. [PubMed: 12963965]
29. Yin XL, Pang JC, Ng HK. Identification of a region of homozygous deletion on 8p22-23.1 in medulloblastoma. Oncogene. 2002; 21:1461–8. [PubMed: 11857089]

30. Yuan BZ, Jefferson AM, Baldwin KT, et al. DLC-1 operates as a tumor suppressor gene in human non-small cell lung carcinomas. Oncogene. 2004; 23:1405–11. [PubMed: 14661059]
31. Wong CM, Lee JM, Ching YP, et al. Genetic and epigenetic alterations of DLC-1 gene in hepatocellular carcinoma. Cancer Res. 2003; 63:7646–51. [PubMed: 14633684]
32. Kim TY, Jong HS, Song SH, et al. Transcriptional silencing of the DLC-1 tumor suppressor gene by epigenetic mechanism in gastric cancer cells. Oncogene. 2003; 22:3943–51. [PubMed: 12813468]
33. Hui AB, Takano H, Lo KW, et al. Identification of a novel homozygous deletion region at 6q23.1 in medulloblastomas using high-resolution array comparative genomic hybridization analysis. Clin Cancer Res. 2005; 11:4707–16. [PubMed: 16000565]
34. Zheng PP, Pang JC, Hui AB, et al. Comparative genomic hybridization detects losses of chromosomes 22 and 16 as the most common recurrent genetic alterations in primary ependymomas. Cancer Genet Cytogenet. 2000; 122:18–25. [PubMed: 11104027]
35. Tong CY, Zheng PP, Pang JC, et al. Identification of novel regions of allelic loss in ependymomas by high-resolution allelotyping with 384 microsatellite markers. J Neurosurg. 2001; 95:9–14. [PubMed: 11453403]
36. Cogen PH, Daneshvar L, Metzger AK, et al. Deletion mapping of the medulloblastoma locus on chromosome 17p. Genomics. 1990; 8:279–85. [PubMed: 1979050]
37. Scheurlen WG, Schwabe GC, Seranski P, et al. Mapping of the breakpoints on the short arm of chromosome 17 in neoplasms with an i(17q). Genes Chromosomes Cancer. 1999; 25:230–40. [PubMed: 10379869]
38. Timmermann B, Kortmann RD, Kuhl J, et al. Role of radiotherapy in the treatment of supratentorial primitive neuroectodermal tumors in childhood: results of the prospective German brain tumor trials HIT 88/89 and 91. J Clin Oncol. 2002; 20:842–9. [PubMed: 11821469]

Europe PMC Funders Author Manuscripts

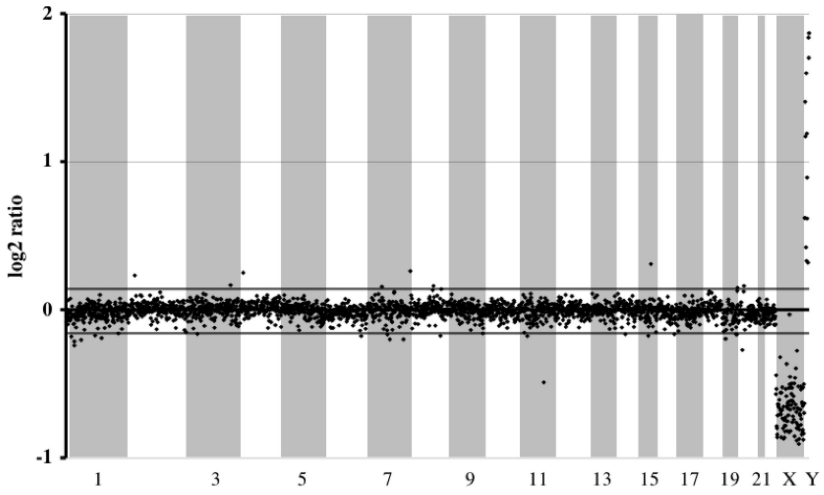

Figure 1. Demonstration of the ability of the array to detect single copy loss and gain

The $\log_2$ ratio of test/reference fluorescence is shown for a normal male (Cy5) versus normal female (Cy3) hybridisation. Clones are arranged in genomic order from 1pter (left) to Yqter (right). The horizontal lines parallel to the y=0 line represent the $\log_2$ values of the mean +/− 3 standard deviations of fluorescence ratios of all autosomal clones in several normal-normal hybridisations. The X clones show loss and Y clones show gain in this male (test) vs female (ref) hybridisation.

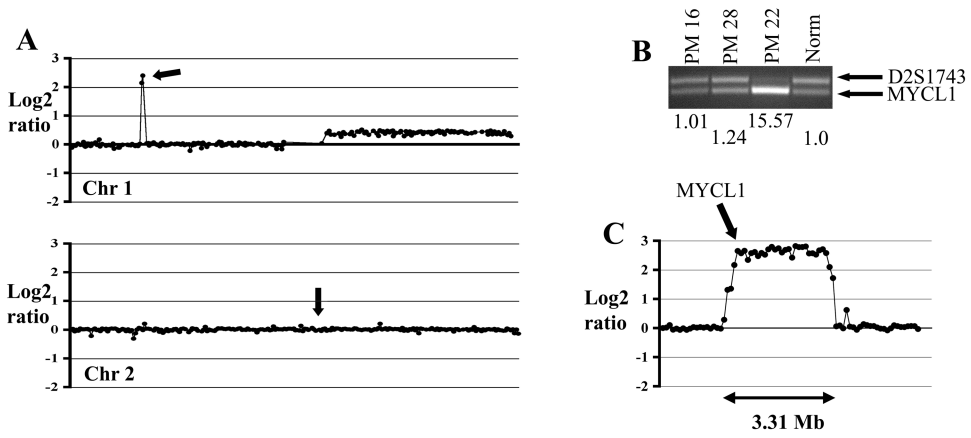

Figure 2. High-level amplification of *MYCL1*

(A) High-level amplification of 2 adjacent clones was seen on 1 Mb array CGH. Semi-quantitative multiplex PCR was performed using primers for exon 2 of *MYCL1* (A, top figure, arrow) and a control locus, D2S1743 (A, bottom figure, arrow) which did not show copy number change. Clones are depicted from pter (far left) to qter (far right) (B) *MYCL1*:control intensity ratios are shown following normalisation to the control constitutional DNA ratio ('Norm'). PM 22 showed high-level amplification of exon 2 of *MYCL1.* (C) A tile-path array of the region confirmed a 3.31 Mb amplicon containing *MYCL1* (position arrowed). The clones used are listed in Supplemental Data 2.

Europe PMC Funders Author Manuscripts

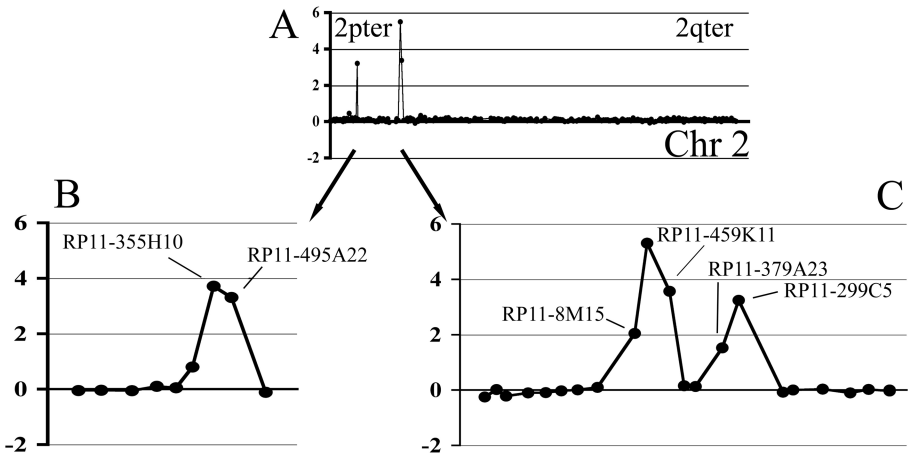

Figure 3. High-level amplifications on chromosome 2

Case PM34 had two separate amplicons on chromosome 2. Log_2 normalised Cy5:Cy3 intensity ratios (ordinate) are plotted against clone position (abscissa) from 2p telomere (far left) to 2q telomere (far right). (B) Tiling path array CGH of the first amplicon showed amplification of clones RP11-355H10 and RP11-495A22, encoding the oncogenes *MYCN* and *MYCNOS*. (C) The larger amplicon was composed of 2 smaller amplicons containing several genes, detailed in Table 1.

Europe PMC Funders Author Manuscripts

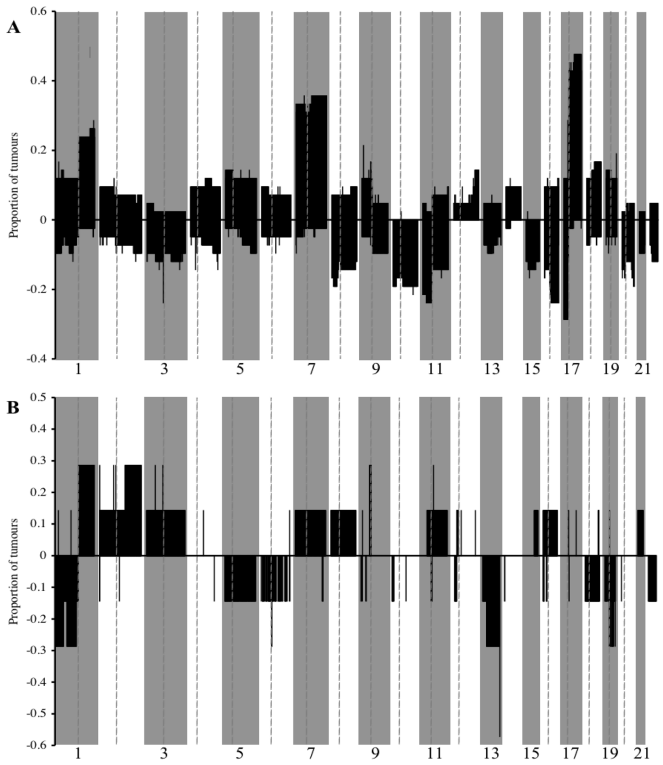

Figure 4. Summary of the gains and losses found in all tumours examined

Clones are plotted along the x-axis in genomic order, from 1pter (left) to 22qter (right). The y-axis shows the proportion of tumours to show gain (above the x-axis) or loss (below the x-axis) of each clone. (A) shows the results for medulloblastomas; (B) shows the same plot for supratentorial PNETs. Alternating light and dark bands denote chromosomal boundaries; vertical hashed lines represent centromeric position.

Europe PMC Funders Author Manuscripts

Europe PMC Funders Author Manuscripts

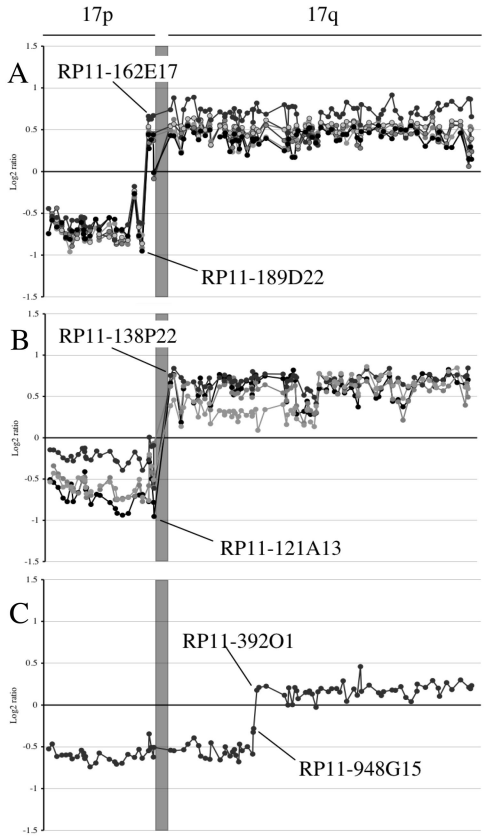

Figure 5. Breakpoints seen in cases with isochromosome 17q

Plots show the three discrete breakpoints seen in cases with findings suggestive of isochromosome 17q. Log_2 ratio of all chromosome 17 clones is shown from 17pter (left) to 17qter (right). Each plot represents one case. The shaded box represents the centromeric clone gap. The most common breakpoint, shown in (A), lay between clones RP11-189D22 and RP1-162E17 on 17p11.2 (n=6). The second main breakpoint (n=4), shown in (B), was peri-centromeric, between clones RP11-121A13 (17p11.2) and RP11-138P22 (17q11.2). One further case (C) had a breakpoint on 17q21.31, between clones RP11-948G15 and RP11-392O1. In the majority of cases when visualised on a log_2 scale, 17p loss was more pronounced than 17q gain. This is in accord with the expected log_2 ratio for single copy loss (-1.0) and single copy gain (+0.58) in a near-diploid sample. In practice there was a tendency for ratios to be closer to zero for reasons such as normal cell ‘contamination’.

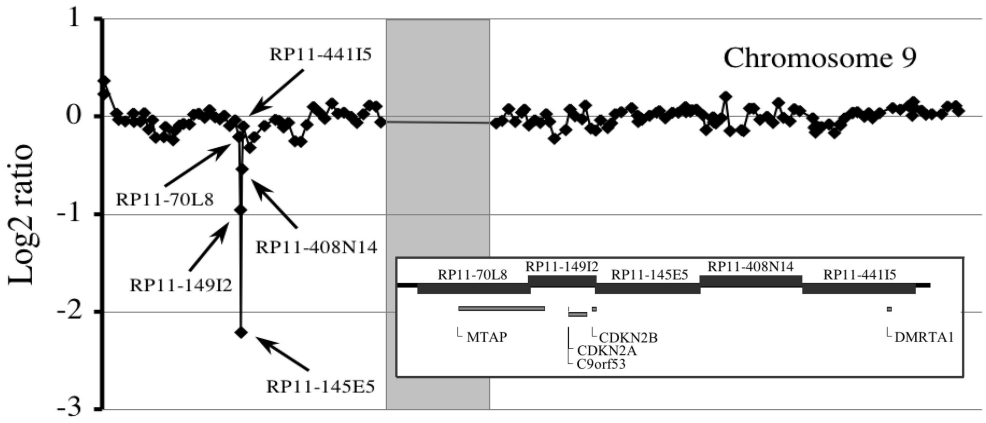

Figure 6. Homozygous loss of the tumour suppressor genes CDKN2A and CDKN2B

Case PM 20 shows homozygous loss of a single clone, RP11-145E5 (log_2 ratio −2.21) at 9p21.3 encompassing the *CDKN2A* and *CDKN2B* genes, surrounded by single copy loss of a 0.4Mb region defined by clones RP11-149I2 to RP11-408N14. The figure layout is as for Figure 3.

Europe PMC Funders Author Manuscripts

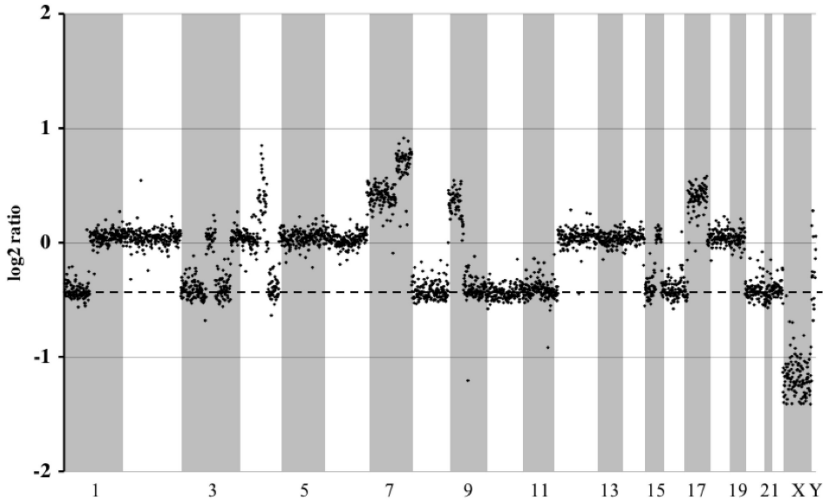

Figure 7. Clarification of modal copy number using interphase FISH

Array CGH of PM 35 revealed a $\log_2$ ratio close to zero for the majority of 1q, 2, 5, 6, 12, 13, 14, 18 and 19 while 1p, 8, 9q, 10, 11, 16, 20, 21 and 22 had a $\log_2$ ratio of roughly −0.4 (shown by the hashed line). Interphase FISH was performed for this case, using centromeric alpha satellite probes for chromosomes 7, 10, 17 and 18. Chromosome 10, with a mean $\log_2$ ratio of −0.4, was seen to have 2 copies on FISH while chromosome 7, 17 and 18 all had copy numbers of greater than 2. Thus, combining the results of I-FISH and array CGH, genomic regions lying along the hashed line were disomic; all other chromosomal regions showed copy number gain.

Europe PMC Funders Author Manuscripts

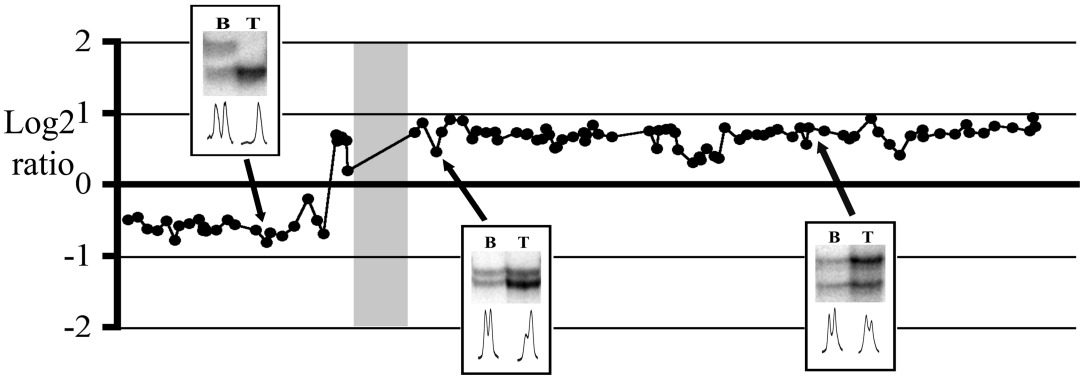

Figure 8. Comparison of array CGH and microsatellite analysis

Array CGH of case PM 10 showed loss of Ch 17: pter-18114679 and gain of Ch 17:19126535-qter. Layout is as for Figure 3. While microsatellite analysis of this case corroborated the array CGH findings, showing partial allelic imbalance at loci on 17q and and complete imbalance on 17p , it was not capable of differentiating loss from gain. Some microsatellite loci are not shown for clarity. In all examples of microsatellite data, blood (B) is shown on the left and tumour (T) on the right, both in gel images and densitometric profiles.

Europe PMC Funders Author Manuscripts

J Neuropathol Exp Neurol. Author manuscript; available in PMC 2010 February 04.

Table 1

Results of semi-quantitative multiplex PCR of genes shown to be amplified by 1 Mb array CGH and tile-path array CGH of the regions surrounding amplified clones

Case	Chromosome	1 Mb clones amplified	Tilepath clones amplified	Length of amplicon	Genes involved in amplicon		Maximum $\log_2$ ratio	Copy number estimated from multiplex PCR[†]
PM 22	1	RP1-118J21 RP4-739H11	RP1-144F13 to RP4-692D3[*]	3.31 Mb	BMP8B CAP1 CITED4 COL9A2 CTPS EDN2 GUCA2A GUCA2B HEYL HIVEP3 HPCAL4 KCNQ4 MYCL1	NFYC NT5C1A OXCT2 PPIE PPIH PPT1 RIMS3 RLF SCMH1 TRIT1 ZMPSTE24 ZMYND12	2.8	31
PM 34	2	RP11-355H10	RP11-355H10 RP11-495A22	230.9 kb	MYCN	MYCNOS	3.7	nd
		RP11-299C5 RP11-478M12	RP11-8M15 RP11-478M12 RP11-459K11	390.3 kb		-	5.3	nd
			RP11-379A23 RP11-299C5	278.9 kb	EML4 COX7A2L	KCNG3	3.2	nd
PM 3	4	RP11-157C8 RP11-18M17 RP11-12J3 RP11-231C18	RP11-4K13 to RP11-238M7[*]	1.81 Mb	FIP1L1 LNX CHIC2	PDGFRA KIT	3.3	15
PM 36	6	RP11-13J16	RP11-13J16 RP4-668J24 RP11-157J24	271.5 kb	FOXQ1	FOXF2	3.5	nd
		RP1-32B1	RP3-352A20 to RP11-371H1[*]	1.19 Mb	ALDH8A1 HBS1L MYB	AHI1 PDE7B	4.0	34
		RP11-3B11	RP11-439F21 to RP11-106E7[*]	778.3 kb	PHACTR2 PLAGL1 SF3B5	STX11 UTRN	3.5	nd
PM 51	19	CTD-2337J16	RP11-351G16 CTD-2337J16	356.2 kb	CACNG8 CACNG6 NDUFA3 PRPF31	LENG1 TMC4 LENG4 RPS9	1.51	nd

Europe PMC Funders Author Manuscripts

Case	Chromosome	1 Mb clones amplified	Tilepath clones amplified	Length of amplicon	Genes involved in amplicon		Maximum log_2 ratio	Copy number estimated from multiplex PCR[†]
					CNOT3	LILRB5		

[*] range refers the clone sets described in Supplemental Data 2. All tile-path clones between these limits were amplified.

[†] calculated according to the formula in Materials and Methods CGH, comparative genomic hybridisation; PCR, polymerase chain reaction; ND, not done.

Europe PMC Funders Author Manuscripts

Table 2

Consistent copy number changes in medulloblastomas and supratentorial PNETs

Chromosomal region	Base pair position	Limiting clones	Length of segment	Affected cases	
Frequently lost in medulloblastomas				Number	%
3p	3: 82655791 - 84801874	RP11-206J21 to RP11-474M18	2.17 Mb	9	27
8p	8: 5106141 - 24469396	RP11-29A2 to RP11-561E1	19.38 Mb	9	27
10p	10: 10pter - 20189475	CTC-306F7 to RP11-188P8	19.92 Mb	9	27
10q	10: 60813485 - 133778458	RP11-357A18 to RP11-45A17	72.99 Mb	8	23
11p	11: 16626917 - 47386308	RP11-4B7 to RP11-125F14	30.78 Mb	10	29
16q	16: 68164911 – 16qter	RP11-311C24 to CTB-121I4	20.41 Mb	10	29
17p	17: 17pter - 19251679	RP11-216P6 to RP1-162E17	18.47 Mb	12	35
20q	20: 52483567 – 20qter	RP11-6L15 to CTB-81F12	9.93 Mb	7	21
Frequently gained in medulloblastomas					
1q	1: 211370717 – 1qter	RP11-323K10 to CTB-160H23	33.97 Mb	11	32
5p	5: 5pter - 45708383	All clones	43.16 Mb	7	21
12q	12: 112632128 – 12qter	RP11-438N16 to RP11-46H11	19.53 Mb	6	18
7q	7: 105390613 - 158432707	RP11-22N19 to CTB-3K23	53.02 Mb	15	44
9p	9: 5993678 - 8490985	RP11-218I7 to RP11-175E13	2.52 Mb	9	27
17q	17: 50112652 – 17qter	RP11-372K20 to RP11-567O16	28.28 Mb	20	59
18q	18: 41216566 – 18qter	RP11-463D17 to CTC-964M9	34.74 Mb	8	24
19p	19: 19pter - 23732307	CTC-546C11 to RP11-359H18	23.54 Mb	6	18
19q	19: 38091322 - 19qter	RP11-298M15 to GS1-1129C9	25.70 Mb	6	18
Frequently lost in supratentorial PNETs					
13q	13: 112739429 – 13qter	RP11-265C7 to RP11-245B11	1.18 Mb	4	57

Number (%) of cases are shown for changes occurring in more than 5 (15%) medulloblastomas and more than 2 (25%) supratentorial PNETs.

BAC and PAC clones denoting the borders of the minimal commonly affected regions of loss and gain are shown in each case.